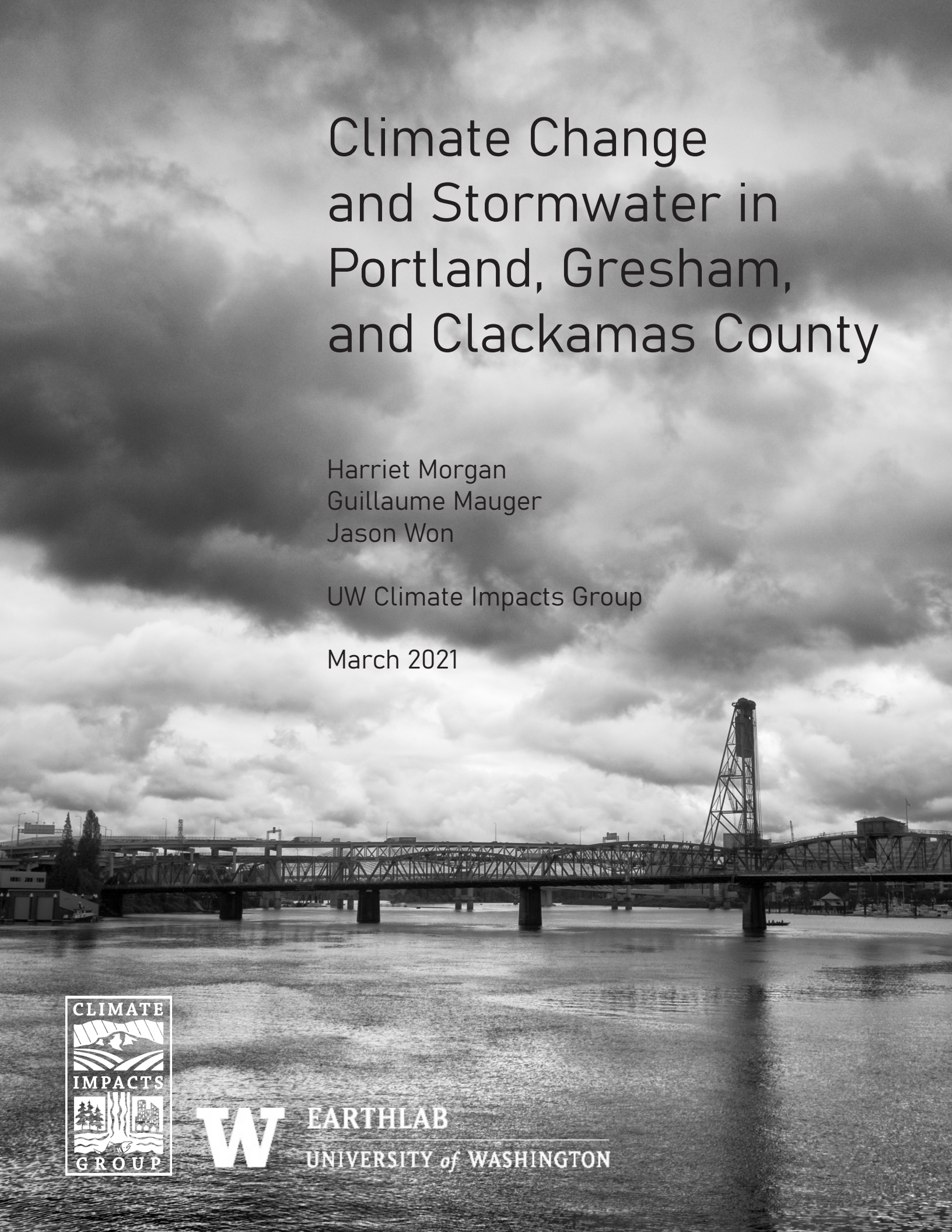

Climate Change and Stormwater in Portland, Gresham, and Clackamas County

Harriet Morgan
Guillaume Mauger
Jason Won

UW Climate Impacts Group

March 2021

CLIMATE IMPACTS GROUP

EARTHLAB
UNIVERSITY of WASHINGTON

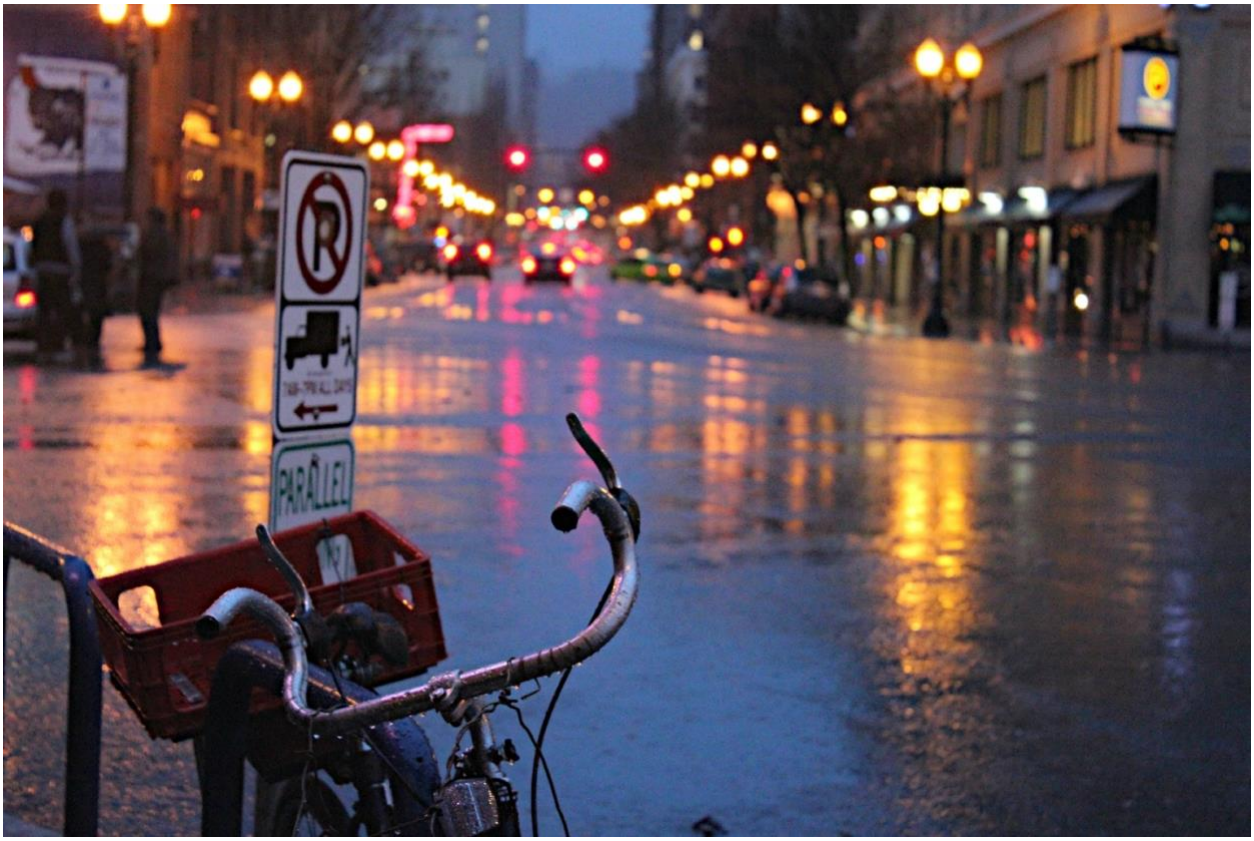

Downtown Portland. Photo by Flickr user Mikal Marquez: https://flic.kr/p/cDf66G

COVER PAGE PHOTO CREDIT: Portland Rain by Grant Matthews, used CC BY-NC-ND 2.0

CITATION:

Morgan, H., G.S. Mauger, and J.S. Won. 2021. Climate Change in Portland, Gresham, and Clackamas County. Report prepared for the City of Portland, City of Gresham, and Clackamas County. Climate Impacts Group, University of Washington.

ACKNOWLEDGEMENTS:

This work was funded by Portland's Bureau of Environmental Services, Clackamas County, and the City of Gresham. The authors would like to thank Cliff Mass, Rick Steed, and Jeff Baars for producing the bulk of the WRF simulations used in this report.

We also received substantial input from a variety of stormwater professionals on the design and purpose of the visualizations, and would like to thank the following individuals for their help:

- Nishant Parulekar, City of Portland
- Kaitlin Lovell, City of Portland
- Nicholas McCullar, City of Portland
- Gregory Savage, City of Portland
- Lisa Huntington, City of Portland
- Tim Kurtz, City of Portland
- Kate Carone, City of Portland
- Ronald Clackamas County
- Torrey Lindbo, City of Gresham
- Katie Holzer, City of Gresham
- Robert Stahle, City of Gresham
- Mark Maurer, Thurston County
- Nat Kale, Thurston County
- Sam Phillips, Port Gamble S'Klallam Tribe
- Paul McCollum, Port Gamble S'Klallam Tribe
- Souheil Nasr, City of Everett
- Lara Whitely Binder, King County
- Jeff Burkey, King County
- Bob Swarner, King County
- Shaun O'Neil, King County

TABLE OF CONTENTS

Executive Summary

Recent research suggests that future heavy rain events will be more intense in the Pacific Northwest (e.g., Warner et al. 2015). Past studies have not accounted for this change, either because the methods cannot reliably capture changes in rainfall intensity (e.g., Abatzoglou and Brown 2012), or because previous studies did not evaluate changes in short-duration precipitation (e.g., hourly) that are of relevance to stormwater planning (e.g., Salathé et al. 2010).

The purpose of this project was to develop projections of 21st century changes in precipitation that can be used to inform stormwater and wastewater management in the cities of Portland and Gresham, and Clackamas County.

Our results show the potential for large increases in future rainfall intensity. For example, models project an increase of +32% (range: -1% to +94%) for the 10-year event with a 1-hour duration at Portland Airport. Results differ by location, metric, and duration; generally showing a larger change for the more extreme events (e.g., the projected change for the 25-year is generally larger than that for the 2-year event) and for shorter durations (e.g., the projected increase for 1-hour events is generally greater than for 24-hour events).

We developed an interactive visualization for browsing the results, based on feedback and testing with prospective users (Figure ES-1). The tool can be used to

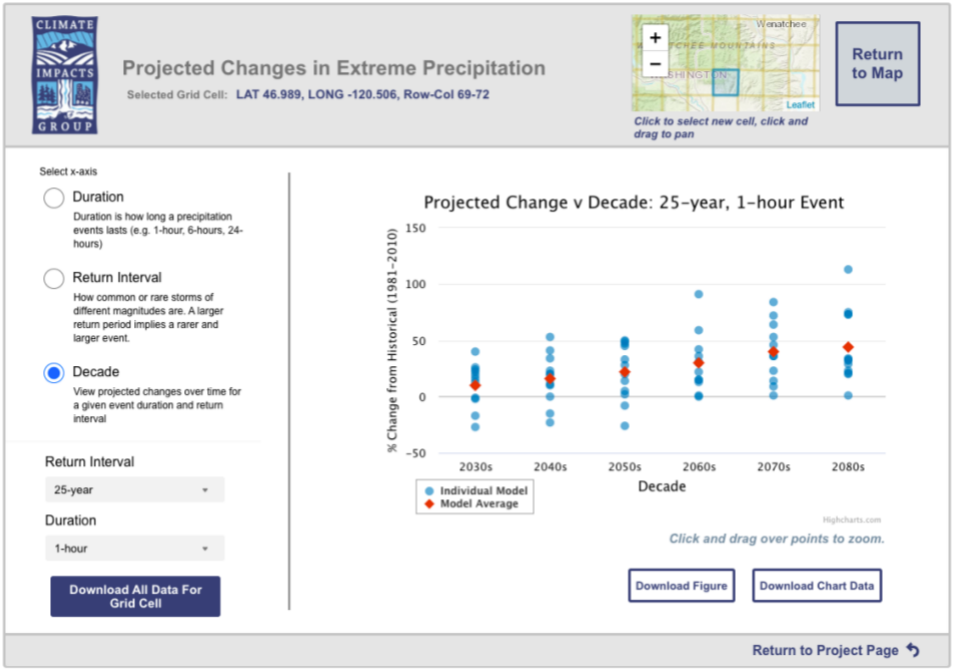

Figure ES-1. Screenshot of the interactive visualization developed to allow quick access to the results for a specific grid cell. The tool can be accessed via the project website: https://cig.uw.edu/projects/heavy-precipitation-projections-for-use-in-stormwater-planning/

browse results for any location within the full model domain, allowing users to quickly view results and download images and data for offline use.

Additional data is made available at specific rain gauge sites for use in continuous stormwater modeling or other more detailed analyses. All data, documentation, and findings are made available online, including an interactive tool that allows users to easily navigate to the station and results of interest.

Background

Changes in the intensity, duration, and frequency of precipitation may negatively affect stormwater and wastewater facilities, exacerbate landslide and urban flood risk, and lead to other public safety and water quality concerns. Recent research has shown that heavy rain events are projected to become more intense with climate change (e.g., Warner et al. 2015, Trenberth 2011).

Previous research suggested very little projected change in precipitation for the region. This is in part due to new methods of "downscaling" the large-scale changes projected by global climate models (GCMs) to smaller-scale changes of relevance to impacts assessment. Studies have shown that a physics-based approach ("dynamical downscaling"), is needed to capture changes in precipitation extremes and the associated impacts (Salathé et al. 2014). Previous approaches relied primarily on an empirical approach ("statistical downscaling"), which does not provide reliable estimates of changes in precipitation extremes. In dynamical downscaling, a regional climate model is used to simulate local-scale changes in climate, leading to a better representation of changes in the physical processes at these smaller scales. This distinction is particularly important for precipitation, since dynamical downscaling can explicitly represent the interactions of weather systems with the complex terrain of the Pacific Northwest.

Regional weather and climate patterns can be influenced by conditions in other parts of the globe. As a result, regional climate model (RCM) simulations can only be produced by using the outputs from a GCM as boundary conditions (i.e.: meteorological conditions at the edges of the model domain). Heavy rain events in the Pacific Northwest are typically driven by "Atmospheric River" (AR) events, in which narrow bands of concentrated moisture are carried into the region from lower latitudes. Previous studies have shown that global models are capable of representing the key aspects of Atmospheric Rivers (e.g., Flato et al., 2014), but lack the resolution to capture the local consequences for precipitation given the complex topography of the Pacific Northwest. This means that: (1) RCMs are needed to estimate local-scale changes in extreme precipitation, and (2) global climate models are appropriate to use as boundary conditions for these regional climate simulations.

Cliff Mass, in University of Washington's Department of Atmospheric Sciences, recently produced an ensemble of new RCM projections for the Pacific Northwest region. These new projections are the basis for the results described in this report.

Global Climate Model (GCM) Projections

GCM projections were obtained from the Climate Model Inter-comparison Project, phase 5 (CMIP5; Taylor et al., 2012). As part of the CMIP5 project, international modeling groups coordinate to create a set of consistent future simulations, driven by predetermined greenhouse gas scenarios ("Representative Concentration Pathways", or RCPs, van Vuuren et al. 2011; for more information see Section 1 of Mauger et al., 2015). The new regional climate model ensemble includes 12 GCMs, chosen based on Brewer et al. (2016) and listed in Table 1. There are 13 projections: 12 based on the high-end RCP 8.5 scenario (Van Vuuren et al., 2011), and a one for the low-end RCP 4.5 scenario for the ACCESS 1.0 model. This means that there are two ACCESS 1.0 projections: one each for RCP 4.5 and RCP 8.5.

The selection of models listed in Table 1 differs substantially from those identified in previous CMIP5 GCM evaluations (e.g., Rupp et al., 2013; Mauger et al., 2018). Specifically, ACCESS 1.3 was not evaluated by Mauger et al. (2018). Of the other models, only four (ACCESS1-0, CanESM2, GFDL-CM3, and NorESM1-M) were retained as the top-performing models in that analysis. Similarly, of the top 10 GCMs selected by Rupp et al. (2013), Table 1 only includes three GCMs (CCSM4, CSIRO-Mk3-6-0, and CanESM2). This is a well-known limitation of GCM evaluation: Previous research has shown that model ranking can differ substantially depending on the criteria used for GCM evaluation (e.g., Brekke et al. 2008). Fortunately, the Brekke et al. findings also suggest that ensembles of more than 6-10 models tend to converge on the same average projection: both in terms of the average change and the range among models. Although the range in any model ensemble is likely related to the true uncertainty in future precipitation extremes, it is important to bear in mind that it is an approximation of the uncertainty, since individual GCMs are not fully independent and are unlikely to span the full range of uncertainties. In addition, the range among RCM projections is influenced by both the uncertainty in GCM projections *and* the additional uncertainties introduced by the RCM.

Table 1. Global climate models (GCMs) used as input to the regional model simulations. All simulations are based on the high-end RCP 8.5 greenhouse gas scenario (Van Vuuren et al., 2011).

Model	Center	Resolution	Vertical Levels
ACCESS1-0	Commonwealth Scientific and Industrial Research Organization (CSIRO), Australia/ Bureau of Meteorology, Australia	1.25 x 1.88	38
ACCESS1-3	Commonwealth Scientific and Industrial Research Organization (CSIRO), Australia/ Bureau of Meteorology, Australia	1.25 x 1.88	38
bcc-csm1-1	Beijing Climate Center (BCC), China Meteorological Administration	2.8 × 2.8	26
CanESM2	Canadian Centre for Climate Modeling and Analysis	2.8 × 2.8	35
CCSM4	National Center of Atmospheric Research (NCAR), USA	1.25 × 0.94	26
CSIRO-Mk3-6-0	Commonwealth Scientific and Industrial Research Organization (CSIRO) / Queensland Climate Change Centre of Excellence, Australia	1.8 × 1.8	18
FGOALS-g2	LASG, Institute of Atmospheric Physics, Chinese Academy of Sciences	2.8 × 2.8	26
GFDL-CM3	NOAA Geophysical Fluid Dynamics Laboratory, USA	2.5 × 2.0	48
GISS-E2-H	NASA Goddard Institute for Space Studies, USA	2.5 × 2.0	40
MIROC5	Atmosphere and Ocean Research Institute (The University of Tokyo), National Institute for Environmental Studies, and Japan Agency for Marine-Earth Science and Technology	1.4 × 1.4	40
MRI-CGCM3	Meteorological Research Institute, Japan	1.1 × 1.1	48
NorESM1-M	Norwegian Climate Center, Norway	2.5 × 1.9	26

Regional Climate Model Simulations

RCM simulations were performed using the Weather Research and Forecasting (WRF, http://www.wrf-model.org; Skamarock et al., 2005) community mesoscale model. WRF is a nonhydrostatic and mesoscale numerical weather model.

Simulations were performed using WRF version 3.2 implemented following Salathé et al. (2010, 2014). Initial and boundary conditions were provided by the GCMs listed in Table 1. Lateral boundary conditions and sea surface temperature (SST) were updated once every six hours.

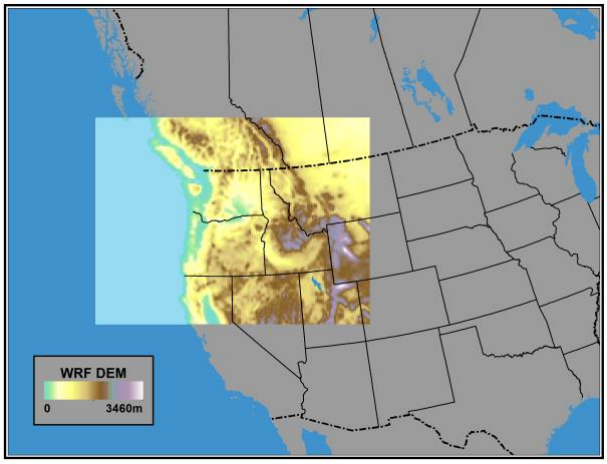

Figure 1. Inner domain for the WRF model, at a spatial resolution of 12 km.

Projections were downscaled to the region using two nested domains (Figure 1). The outermost domain at 36-km resolution covers the western North American continent and much of the eastern Pacific Ocean, in order to capture the climatological western flow and the evolution of approaching ARs. The innermost domain, at 12-km resolution, encompasses the U.S. Pacific Northwest. One-way nesting was applied in this study.

Thirty vertical levels were used in the model spanning from the surface to 10 hPa, with the finest vertical resolution in the boundary layer. WRF runs were initialized three months prior to the start date of each simulation as spin-up. The physics parameterizations for microphysics, cumulus parameterization, planetary boundary layer, land surface models, and longwave and shortwave radiation are summarized in Lorente et al. (2018). Although we did not perform an extensive validation of the model's performance, previous research has established that it captures the essential characteristics of local-scale weather variations in the Pacific Northwest (e.g., Dulière et al. 2011).

Simulations were performed for the years 1970 through 2099. Results were archived at hourly intervals following Greenwich Mean Time (GMT, which is 8 hours ahead of local standard time in the Pacific Northwest).

Observations

Hourly precipitation observations were obtained from three datasets:

1. The HYDRA Rainfall Network, operated and maintained by the city of Portland Bureau of Environmental Services (https://or.water.usgs.gov/precip/)
2. The NOAA Hourly Precipitation Dataset, version 2 (HPDv2; Wuertz et al., 2018; https://www.ncei.noaa.gov/data/coop-hourly-precipitation/v2/).
3. The NOAA Local Climatology Dataset (LCD; https://www.ncdc.noaa.gov/cdo-web/datatools/lcd)

Stations in the vicinity of Portland, Gresham, and Clackamas County are shown in Figure 2 and Table 2; the full list of stations in all of Oregon and Washington is in the Appendix. All data were obtained at an hourly time step. Values were converted to millimeters (mm) for the analysis. Rain gauge observations from the HYDRA network are quality controlled by City of Portland staff. The only additional quality control that was applied to these gauges was to limit the analysis to gauges for which observations continue through at least 1995 and had at least 10 years of valid data (see definitions below).

Additional observations of hourly precipitation were obtained from NOAA's HPDv2 rain gauge sites and airport observations from the LCD network through the NOAA National Center for Environmental Information (NCEI) website. The HPD dataset stems from the NOAA / National Weather Service Fischer-Porter rain gauge network, consisting of approximately 1900 gauges across the country, with some records extending back to the 1940s. The new version 2 dataset, HPDv2, transitioned the approach from manual to automated data acquisition and quality control. LCD data primarily comes from Automated Surface/Weather Observing Systems (ASOS/AWOS) located at airports; we include this data here specifically to ensure data are available at key regional airports with sufficient data.

In order to ensure enough data were available for the analysis, at times that overlap with the RCM simulations, the following criteria were used for selecting which NOAA HPD and LCD stations to include:

1. At least 30 years from start to end of the observational record,
2. At least 10 years of valid data, where a year is counted as "valid" if 90% of observations are available for each month in the year, and
3. Observations continue through at least 1995.

In all, there were 53 HYDRA, 75 HPD, and 10 LCD stations that met these criteria. All gauges are listed in the Appendix, those that are most pertinent to the current study are listed in Table 2.

The HPD data include two quality control flags: a "Measurement" and a "Data Quality" flag. Observations were treated as missing values if any of these flags were present, with one exception: data flagged as trace precipitation ("T") were set to zero (valid data, no precipitation). There are no data quality flags in the LCD data; as with the HPD data, trace precipitation was set to zero. All precipitation data were evaluated to verify that values are within the range of plausible values for hourly precipitation, which we defined as ranging from 0 to 203.2 mm (or 8 inches) in one hour; no values were found to be outside of that range.

Previous work with the HPD dataset data revealed periods when precipitation was zero for long stretches, extending beyond one month without precipitation, yet there were no flags to indicate missing data. Data checks with other gauge networks, showed that dry spells of this length do not occur in the region, even in the relatively drier eastern half of the state. As a result, data were set to missing when all-zeros stretches extended to more than 60 consecutive days.

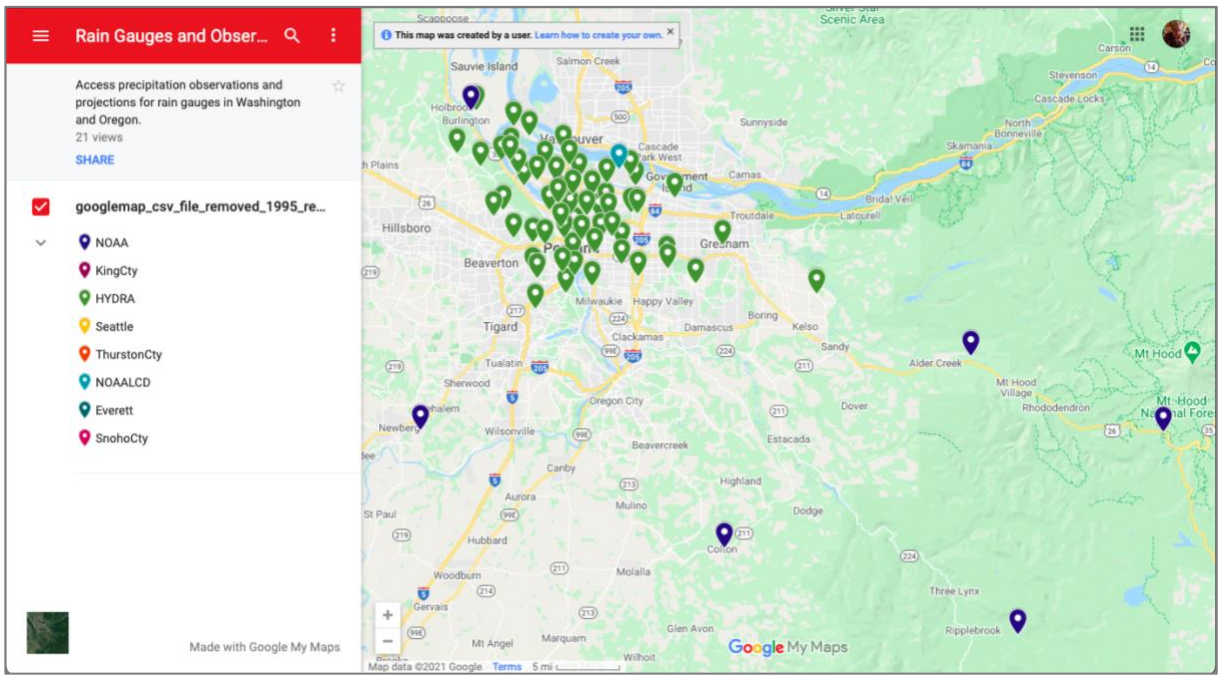

Figure 2. Screenshot showing a map of the stations included in the area encompassing Portland, Gresham, and Clackamas County. This map can be accessed online via the project website: https://cig.uw.edu/projects/heavy-precipitation-projections-for-use-in-stormwater-planning/

By applying these additional criteria, we were able to remove the vast majority of questionable data.

Finally, two data considerations are worth noting. First, many of the HYDRA gauge records are quite short, limiting the accuracy of the precipitation statistics that can be obtained. This is evident in the results that are presented below. As a result, we have limited the analysis to only HYDRA stations with at least 10 years of valid data. Additional work is needed to determine the criteria necessary to ensure an adequate bias correction and explore options for a regionally generalized bias correction. Second, although we have attempted to comprehensively remove errors in the observations, some anomalous values may remain, and these errors could affect the bias correction of the model projections. For this reason, we have included extensive information on the model biases that are present prior to bias correction, in the products outlined below. In addition, **we recommend using the percent changes from the raw projections as opposed to absolute changes from the bias-corrected model projections whenever this is an option**.

Table 2. Rain gauge stations in the area encompassing Portland, Gresham, and Clackamas County. The full list of rain gauges for all of Washington and Oregon is listed in the Appendix.

Network	ID	Name	Lat. / Lon.	Years
NOAA HPD	USC00351033	Brightwood	45.38530N / 122.04580W	1975-2020
NOAA HPD	USC00351735	Colton	45.17280N / 122.43420W	1952-2020
NOAA HPD	USC00352697	Estacada	45.07670N / 121.97140W	1949-2020
NOAA HPD	USC00353402	Government Camp	45.30080N / 121.74250W	1967-2020
NOAA HPD	USC00357127	Rex	45.30330N / 122.91330W	1952-2020
NOAA HPD	USC00357572	Sauvies Island	45.65550N / 122.83380W	1952-2020
NOAA HPD	USC00357823	Silverton	45.00580N / 122.77390W	1963-2020
NOAA LCD	72698024229	Portland Airport	45.59083N / 122.60028W	1936-2020
HYDRA	111	Airport Way PS02	45.55884N / 122.51288W	2000-2019
HYDRA	1	Ankeny FS	45.52210N / 122.67061W	1996-2019
HYDRA	174	Arleta School	45.48620N / 122.59592W	2004-2019
HYDRA	193	Astor School	45.57891N / 122.72971W	2007-2019
HYDRA	152	Beaumont School	45.54869N / 122.62133W	1997-2019
HYDRA	58	Bonny Slope School	45.54546N / 122.78368W	1980-2015
HYDRA	153	Cascade PCC	45.56358N / 122.67352W	1977-2019

Network	ID	Name	Lat. / Lon.	Years
HYDRA	192	Children's Museum	45.50856N / 122.71787W	2007-2018
HYDRA	10	Collins View	45.45410N / 122.68434W	1977-2019
HYDRA	107	Columbia IPS	45.59481N / 122.71731W	1977-2018
HYDRA	144	Columbia STP	45.59479N / 122.71732W	1977-2018
HYDRA	146	Cottrell School	45.45377N / 122.28849W	1989-2019
HYDRA	12	Fernwood	45.53676N / 122.63152W	1979-2011
HYDRA	012F	Fernwood	45.53676N / 122.63152W	1977-2011
HYDRA	72	Fremont PS	45.54217N / 122.57131W	1982-2010
HYDRA	317	Fremont PS	45.54216N / 122.57133W	1982-2010
HYDRA	175	Glencoe ES	45.51682N / 122.61115W	2003-2018
HYDRA	20	Gresham Fire	45.50758N / 122.43732W	1991-2019
HYDRA	125	Guilds PS	45.57305N / 122.75041W	1977-2004
HYDRA	64	Harney PS	45.46229N / 122.64320W	1992-2019
HYDRA	7	Hayden Island PS	45.61202N / 122.68867W	1995-2018
HYDRA	21	Holgate PS	45.48953N / 122.52443W	1992-2012
HYDRA	14	Kelly School	45.47292N / 122.57005W	1979-2019
HYDRA	014F	Kelly School	45.47292N / 122.57005W	1977-2019
HYDRA	130	Linnton PS	45.60060N / 122.78563W	1979-1999
HYDRA	213	Madison HS	45.54333N / 122.58078W	2010-2019
HYDRA	115	Mallory PS	45.58146N / 122.66311W	1996-2019
HYDRA	172	Maplewood ES	45.47066N / 122.73023W	2003-2019
HYDRA	137	Marine Dr PS	45.62796N / 122.74150W	1985-2010
HYDRA	173	Metro Learning Ctr	45.52681N / 122.69324W	2003-2019
HYDRA	6	Mt Tabor Yard	45.50574N / 122.59662W	1977-2018
HYDRA	181	Multnomah Co	45.51270N / 122.66013W	2005-2019
HYDRA	48	Open Meadows	45.57799N / 122.69961W	1996-2018
HYDRA	9	PDX Bus Park PS	45.57260N / 122.57378W	1992-2003
HYDRA	159	PDX Post Office PS	45.58389N / 122.58293W	2005-2019
HYDRA	145	Pleasant Valley	45.46475N / 122.47963W	1977-2019
HYDRA	3	Sauvies Island School	45.65530N / 122.82528W	1978-2011
HYDRA	147	Skyline FS	45.59393N / 122.81848W	1977-2002

Network	ID	Name	Lat. / Lon.	Years
HYDRA	2	Skyline School	45.60784N / 122.85665W	1977-2019
HYDRA	171	Sunnyside School	45.51458N / 122.62925W	2004-2019
HYDRA	164	SW 12th And Clay	45.51517N / 122.68753W	2001-2019
HYDRA	204	Swan Island CSO PS	45.55337N / 122.69606W	2008-2019
HYDRA	122	Swan Island PS	45.55527N / 122.69313W	1995-2007
HYDRA	4	Sylvania PCC	45.43685N / 122.73175W	1977-2019
HYDRA	161	Sylvan School	45.50994N / 122.73700W	2001-2017
HYDRA	167	Terminal 4	45.60076N / 122.77156W	2001-2011
HYDRA	120	Thomas PS	45.49392N / 122.67270W	1996-2009
HYDRA	89	Vermont Hills	45.47704N / 122.73618W	1985-2001
HYDRA	41	Vernon School	45.56243N / 122.64343W	1996-2018
HYDRA	300	West TV School	45.51528N / 122.76712W	1977-1995
HYDRA	160	WPCL	45.58569N / 122.75947W	2001-2019
HYDRA	121	Yeon PS	45.54618N / 122.71031W	1986-2019

Post-Processing and Model Evaluation

WRF data extraction

The WRF outputs are on a curvilinear 12-km grid. The model outputs separate precipitation estimates based on whether it is simulated as a result of the convective parameterization occurring at the sub-grid scale or as part of a large-scale process that is resolved by the model. As is typical, precipitation was calculated as the sum of these two quantities.

Hourly data were extracted for the grid point nearest to each rain gauge station (so-called "nearest-neighbor" interpolation). These constitute the "raw" WRF data for each station dataset. Since the WRF resolution is coarse compared to the spacing of the rain gauge stations, different stations can be associated with the same raw WRF data.

Although WRF projections represent a substantial improvement over previous downscaled precipitation estimates, the simulations do contain biases (e.g., Figure 3). Many applications require estimates of absolute precipitation totals, especially those that involve continuous

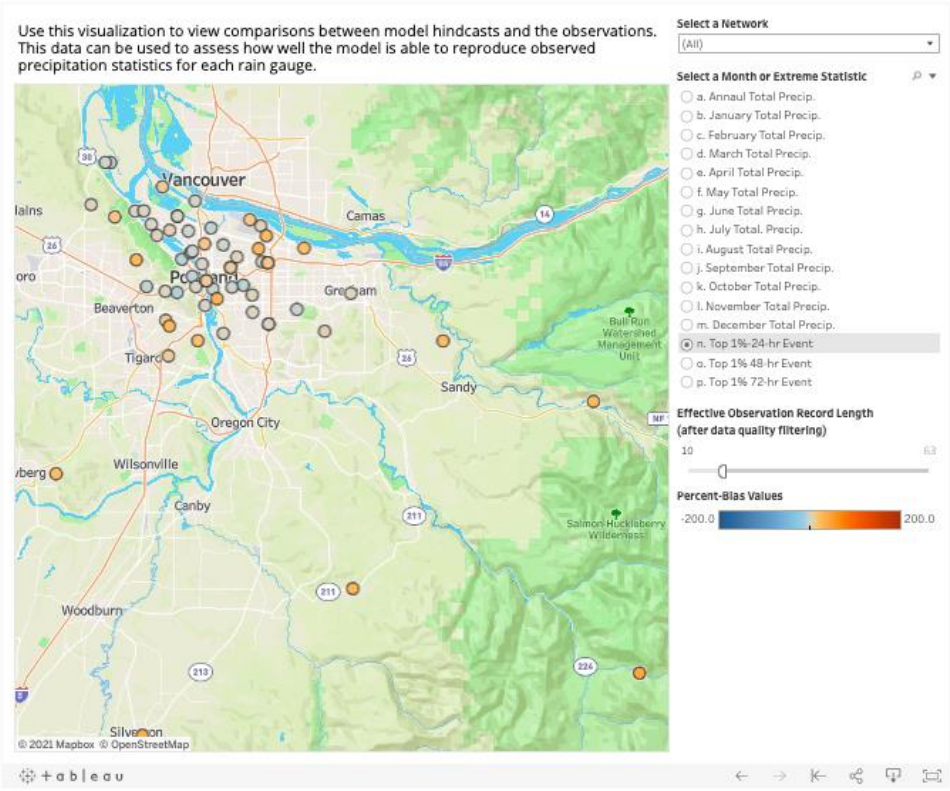

Figure 3. Screenshot showing a map of the percent bias for stations in the area encompassing Portland, Gresham, and Clackamas County. This visualization can be accessed online via the project website: https://cig.uw.edu/projects/heavy-precipitation-projections-for-use-in-stormwater-planning/

simulation of stormwater or other system performance. In these cases, it is not always practical to apply a simple percent change to observed historical precipitation intensities, such as those typically obtained from an intensity-duration-frequency relationship. As a result, the raw WRF data were additionally bias-corrected to match the observations at each rain gauge site.

Bias Correction

For each station location, the raw WRF hourly precipitation was bias corrected to the historical hourly station data. Observed data were quality controlled as described in the previous section, and the full period of record was used for each station.

Although bias correction is a key tool used in many applications, recent work has shown that it can introduce artifacts in the case of climate change, especially when considering changes in extremes (Mauger et al. 2016). For this study, we applied the "Percentile-Delta" method described in Mauger et al. (2018). This approach combines the intensity-based bias correction of the quantile mapping approach with the stability of a simple multiplicative scaling. Specifically, the historical WRF (1970-2005) was compared to the observations to estimate a separate multiplicative scalar for each percentile (i.e., 0-1, 1-2, … 99-100). These same scalars were applied to the future WRF simulations (2006-2099). As described in Mauger et al. (2018), tests indicate that this method reduces model biases without introducing spurious trends.

Summary Statistics

Precipitation totals and extreme statistics were calculated for overlapping 30-year time periods extending through 2099 (Table 3). Projected changes for the future time periods were all assessed relative to the results for the 1990s.

Using 30-year time periods is conventional in climate science as a way of ensuring the sample size is large enough to limit the influence of natural variability, which can cause fluctuations in climate on time scales ranging up to several decades. Although longer time periods could further improve the statistics that are obtained, doing so would limit our ability to detect long-term trends. This is why 30-years is the convention: it provides an

Table 3. Naming convention used to describe 30-year time periods used in the analysis.

"1990s" = 1981-2010
"2030s" = 2020-2049
"2040s" = 2030-2059
"2050s" = 2040-2069
"2060s" = 2050-2079
"2070s" = 2060-2089
"2080s" = 2070-2099

increased sample size while minimizing the obfuscation of long-term trends.

For the observations, another consideration is missing data. Observational records often have missing data resulting from technical malfunctions, scheduled maintenance, or other factors resulting in a temporary halt in observations. Since limited sample size can lead to biases in estimates, precipitation statistics were only calculated from the observations if the following conditions were met:

1. A minimum of 90% valid observations (< 10% missing values) for each month, for all months, to estimate the maximum or total for the water year or seasonal extreme.
2. A minimum of 5 years of valid observations to compute the long-term average (e.g., of total water year precipitation).
3. A minimum 5 years of valid observations to compute the 2-year extreme, 10 years of valid data to compute the 5-, 10-, and 25-year extremes, and 29 years of valid data for the 50- and 100-year extremes.

Extreme Value Analysis

For most stormwater applications, the key metric is the change in specific storm intensities – for example, the 25-year extreme in 1-hour precipitation. Strictly speaking, we should always refer to the annual chance of exceedance (often referred to as "ACE") instead of the return interval, since the probability of a large event in one year is unrelated to whether or not there was one the year before. Table 4 shows how the two terms correspond to one another.

In our analysis, we estimated extreme statistics for the raw regional model projections over the entire model domain, as well as for the raw and bias-corrected data associated with each rain gauge location. In all cases, calculations were applied to multiple precipitation durations ranging from 1 hour to 15 days, and the precipitation intensities estimated for following recurrence intervals: 2-, 5-, 10-, 25-, 50-, and 100-year events (50%, 20%, 10%, 4%, 2%, and 1% annual chance of exceedance, respectively). We computed these

Table 4. Annual Chance of Exceedance corresponding to each return interval. Although more common, return intervals incorrectly imply that events cannot happen more than once in the given interval.

Return Interval (Average)	Annual Chance of Exceedance
2-year event	50%
10-year event	10%
25-year event	4%
50-year event	2%
100-year event	1%
500-year event	0.2%

statistics for the full water year, and also separately for each season (Dec-Feb, Mar-May, Jun-Aug, Sep-Nov) and each calendar month.

The extreme value calculations followed the standard block-maximum approach, fitted to an extreme distribution using L-moments (Hosking and Wallis 2005). To calculate extreme statistics, the Extreme Value type 1 distribution described by Gumbel (EV1), the Log-Pearson type 3 (LP3), and the generalized Extreme Value (GEV) distribution with L-moments are commonly used. In this study we apply the GEV distribution with L-moments to estimate extreme precipitation statistics – following the methodology described in Salathé et al. (2014) and Tohver et al. (2014) – based on findings that indicate it is superior to the LP3 distribution (Rahman et al. 1999 & 2015, Vogel et al. 1993, Millington et al. 2011).

Focus Groups and User Testing

The current work builds on previous work with several Washington State jurisdictions (e.g., King County). In that work we developed a Tableau tool to facilitate access to the extreme precipitation projections. This tool was not intuitive nor was the information accessible to users, likely due to the fact that it was designed and developed without sufficient input and engagement from stormwater managers and engineers and without user design testing to for clarity and interpretability. Through a first round of user-tests with western Washington and Oregon jurisdiction (project sponsors), we gathered information on:

1. *General user needs:* What extreme precipitation information do stormwater managers need? How do we support actions (e.g., from the planning to the project end, whole spectrum, or communications)?
2. *Specific user needs:* How can we modify the Tableau visualization, and the data delivery in general, to increase the usability and accessibility of the technical heavy precipitation projections?

Each conversation lasted for 1 hour. In the second half of each meeting users explored the Tableau tool developed in 2017. Users were provided a link to the tool and were asked to think out loud as they navigated through the tool. CIG researchers did not provide guidance to users, as we were interested in better understanding whether the tool navigation was intuitive and how easily the data could be interpreted by the end user.

A total of six user tests were conducted in 2020. CIG collated feedback from these calls to identify challenges that emerged for multiple users, data interpretation issues or "wish-list features" that users would like to see incorporated in future iterations of the visualization.

Examples of what we heard from multiple users:

- *Challenge:* Navigating between different visualization "tabs" was not readily apparent as an option for individuals not familiar with the tool.
- *Challenge:* Users wanted to see a mean or median value for the 12 regional climate models presented in the visualization; this was not included in the tool.
- *Challenge:* Users had the capability to toggle climate models, however, there was no way to reinstate them once they had been removed.

- *Wish-List:* Data download button to provide a csv of customizable data for a specific grid cell.
- *Wish-List:* Remove data validation tab, which was confusing and would not be used by most users.

The scaffolding for the new stormwater visualization was developed using the information from the six user tests. Mock-ups of different visualization tabs were developed in Figma using dummy data. We then conducted a survey to determine whether the new visualization would meet the needs of stormwater managers, and to provide another opportunity for feedback. This survey consisted of six questions and included a mix of multiple-choice and open-ended questions. The survey was sent to 19 individuals from seven different jurisdictions; 18 individuals responded to the survey, with the following key takeaways:

- Users were interested in BOTH duration and recurrence interval as x-axis parameters (72.2%).
- Users were interested in specific durations for inclusion in the visualization: 1-hr, 2-hr, 6-hr, 24-hr, 72-hr storm durations.
- Users were interested in having the model median or mean displayed in addition to the individual model results.

We used these results to further refine specific features and finalize the draft visualization.

A final user-test session was conducted with project sponsors from each of the three jurisdictions. In this session users were provided with an online draft visualization and invited to provide feedback. Suggested improvements included:

- An easy way to select a different grid cell from main visualization, and
- Unique ID number for each grid cell to facilitate comparison and tracking

These were incorporated into the final design of the tool.

Data and Visualizations

All results and visualizations are linked from the project web page (https://cig.uw.edu/projects/heavy-precipitation-projections-for-use-in-stormwater-planning/).

This project page includes four new interactive visualizations: (1) a visualization for viewing and downloading projected change statistics, (2) an online repository for direct access to data files, (3) a tool for exploring observed precipitation statistics for all rain gauges, and (4) a model evaluation tool for comparing model hindcasts and station observations. These are all described in the sections below.

Interactive Visualization

The interactive visualization (Figure 4) is designed to make it easy to view the projections for each model grid cell. The provides three different options for viewing results:

1. By duration, ranging from 1-hour to 72-hours,
2. By return interval, ranging from the 2-year to the 100-year event, and
3. By decade, ranging from the 2030s to the 2080s.

In each case, users select which parameter from the other two categories to plot. For example, if viewing changes across different durations, the user will select the return interval and future decade for which to view changes for all durations.

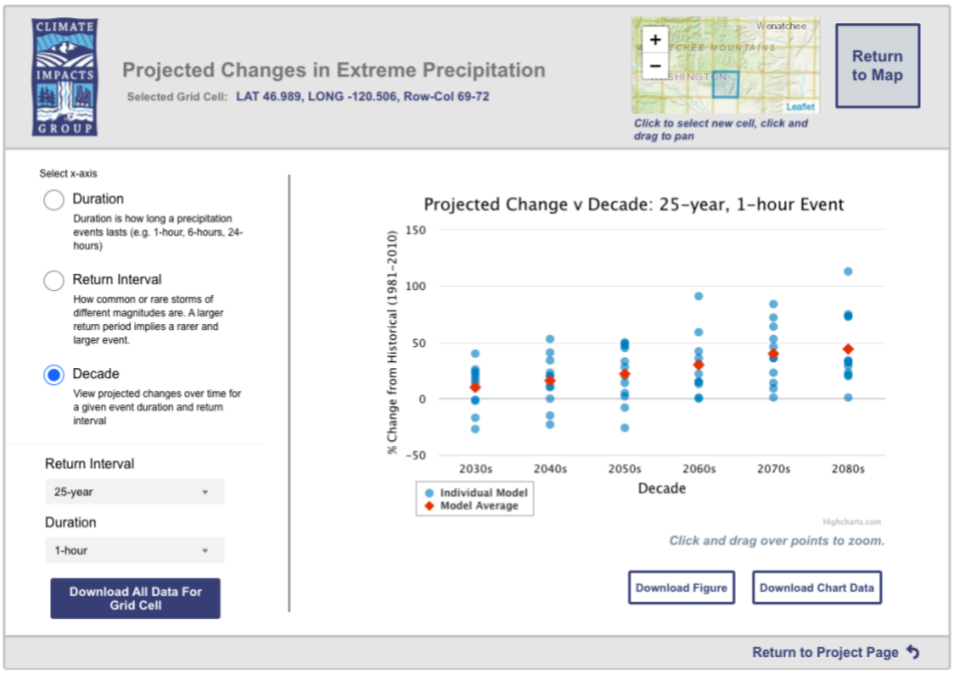

Figure 4. Screenshot of the interactive visualization developed to allow quick access to the results for a specific grid cell. The tool can be accessed via the project website: https://cig.uw.edu/projects/heavy-precipitation-projections-for-use-in-stormwater-planning/

All projections are expressed as the percent change relative to 1981-2010; the time period for the most recent climate normal, following the convention established by NOAA. After selecting the desired options, users can download the figure for later use or download a simple spreadsheet containing the results that are included in the selected chart. Another button allows a user to download all of the data for the selected grid cell. Finally, a thumbnail map at the top of the page makes it easy to browse results for other nearby grid cells.

Online Data Repository

Gridded Data

The data visualization described above draws from a larger archive of projected changes in precipitation extremes, computed for the full WRF domain. These expand on the precipitation statistics that are available in the tool. Specifically, by including more durations (1, 2, 3, 6, 12, 24, 48, 72, 120, 168, 240, and 360 hours) and return intervals (2-, 5-, 10-, 20-, 25-, 50-, and 100-year events) for the precipitation extremes, and by providing statistics for water year extremes as well as for each calendar month and season (Dec-Feb, Mar-May, Jun-Aug, Sep-Nov). For comparison with changes in extremes, we have also calculated the change in total precipitation for the full water year as well as each calendar month and season.

All projections are expressed as a percent change relative to a historical time period. To allow flexibility, we have calculated changes for three separate historical time periods:

1. 1981-2010, with changes assessed for the 2030s, 2040s, 2050s, 2060s, 2070s, and 2080s.
2. 1970-2005, with changes assessed for the 2030s, 2050s, and 2080s.
3. 1970-2015, with changes assessed for 2016-2060 and 2055-2099.

All results are stored as separate Network Common Data Form (NetCDF) files for each GCM projection, with separate files each for the water year, monthly, and seasonal extreme statistics, and another separate set of files for the water year, monthly, and seasonal precipitation totals.

Station-Based Data

The Google Map in Figure 2 provides links to data for each rain gauge site; the organization of the online repository is shown in Figure 5. All files are comma-delimited (.csv), and all values are in millimeters (mm). There are five types of output files, with the following naming conventions:

1. ***Hourly time series files.*** Time series including the full record of observational, raw, and bias-corrected hourly precipitation. For the WRF files these are split into historical (1970-2005) and future (2006-2099) files in order to accommodate the maximum number of rows allowed in Excel. File naming:

   <Network>_<ID>_<lat>_<long>_<raw/bcWRF>_<model>_<scenario>.csv

   <Network>_<ID>_<lat>_<long>_<raw/bcWRF>_<model>_<scenario>.1970-2005.csv

   <Network>_<ID>_<lat>_<long>_<raw/bcWRF>_<model>_<scenario>.2006-2099.csv

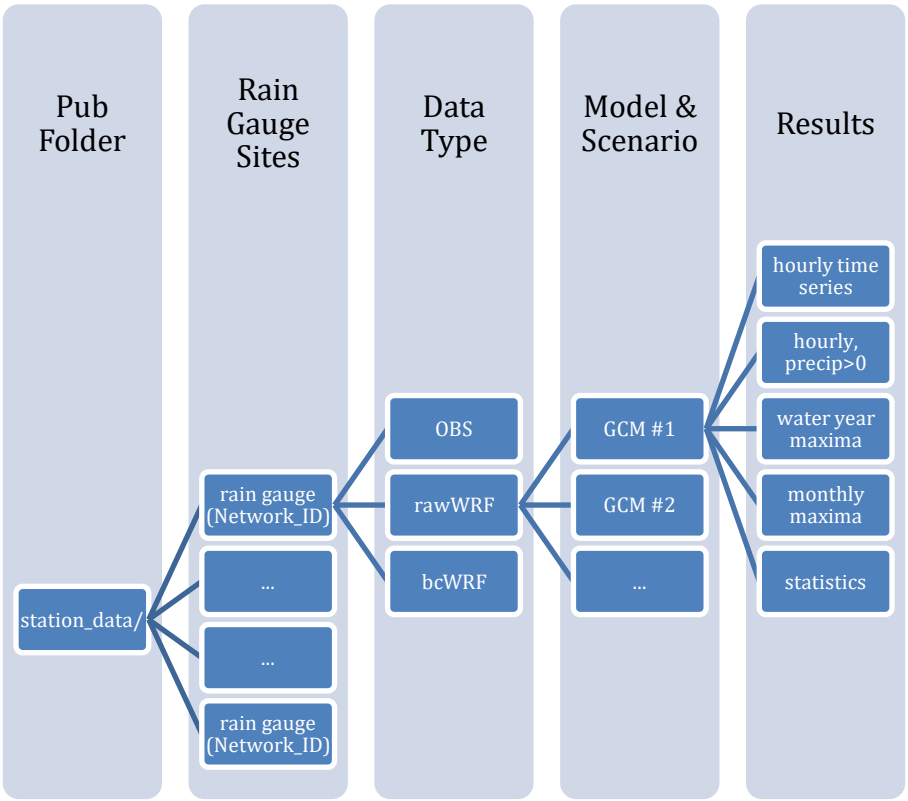

Figure 5. Data structure for the station-based data.

2. ***Time series of non-zero precipitation.*** These are the same as the previous files, except that all zero values of precipitation are removed. For the WRF files, any precipitation value less than 0.001 inch (0.025 mm) were set to zero. File naming:

   <Network>_<ID>_<lat>_<long>_<raw/bcWRF>_<model>_<scenario>.non-zero.csv

3. ***Water year maxima.*** Maximum precipitation for each water year (Oct-Sep), for 11 different durations (1-, 2-, 3-, 6-, 12-, 24-, 48-, 72-, 120-, 240-, and 360-hour precipitation). These are used as the basis for the extremes calculations described in Section 7. File naming:

   <Network>_<ID>_<lat>_<long>_<raw/bcWRF>_<model>_<scenario>.WYmax.csv

4. ***Monthly maxima.*** Same as #3 except showing the maximum for each month. File naming:

   <Network>_<ID>_<lat>_<long>_<raw/bcWRF>_<model>_<scenario>.MOmax.csv

5. ***Extreme Statistics.*** Extreme statistics, for historical and future time periods, for all return intervals and precipitation durations. Two files are included: one listing the absolute totals for each statistic, and another listing the percent change for three future time periods. File naming:

   <Network>_<ID>_<lat>_<long>_<raw/bcWRF>_<model>_<scenario>.stats-abs_vals.csv

   <Network>_<ID>_<lat>_<long>_<raw/bcWRF>_<model>_<scenario>.stats-pct_chg.csv

The observational data file naming is slightly different, since these are not based on a specific model. The file names for these are identical to those listed above, with the following exceptions:

1) The observational data file includes the latitude and longitude of the rain gauge, whereas the WRF files list the position of the nearest model grid point.
2) The WRF-specific suffix '<raw/bcWRF>_<model>_<scenario>' is removed, since it does not apply to the observations.

3) There is no percent change file for the statistics, since future changes are not applicable to the observational record.

Two other tools are meant to provide quick looks at the data associated with each rain gauge. The first, shown in Figure 6, provides the observed rainfall statistics for each gauge. The second tool shows the bias in WRF precipitation, in percent, relative to the measurements at each gauge location. In both cases, results are shown for the same metrics: total precipitation for the year and each calendar month, and the average of the top 1% in precipitation totals for five durations: 1, 2, 6, 24, and 72 hours. In each tool, users can pan and zoom, and hover over each station to view the exact values for each station.

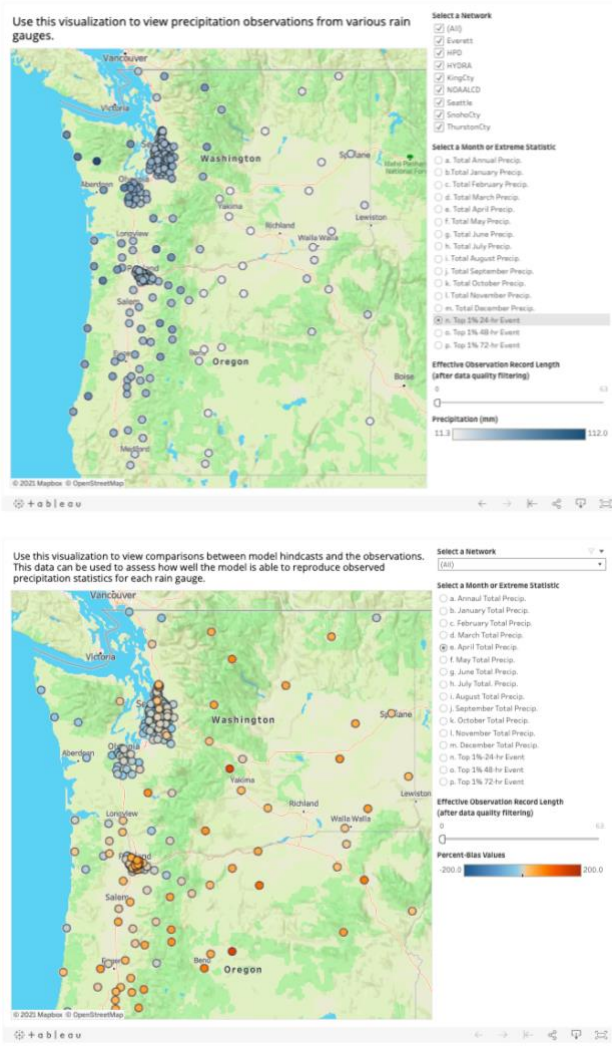

Figure 6. Screenshots of the two tools providing statistics related to each rain gauge station. The top tool provides the observed rainfall averaged over all available observations for each gauge. The bottom tool gives the average bias in the WRF simulation, compared to the observations at that gauge. In both cases, comparisons include all valid observations following the data quality requirements outlined in previous sections of this report. Both tools can be accessed via the project website: https://cig.uw.edu/projects/heavy-precipitation-projections-for-use-in-stormwater-planning/

Results

Projected changes for the grid cell closest to Portland Airport are summarized in Table 5. The table shows results for the 1-hour duration, for the 2080s (2070-2099), relative to 1981-2010. Projections for other precipitation durations (e.g., 2-hour, 6-hour, 24-hour) and time periods (e.g., 2030s, 2050s) are included in the online data and can be browsed in the visualization and the online data repository, described above. Each row in Table 5 shows the results for either the total accumulation (1st row), or for precipitation extremes at different return intervals ranging from the 2- to the 100-year event. Columns show the results for both WRF simulations for the

		Water Year	Dec-Feb	Mar-May	Jun-Aug	Sep-Nov
Total Precip.		**+13%** (+3%, +26%)	**+20%** (+8%, +42%)	**+11%** (-6%, +32%)	**-10%** (-43%, +38%)	**+13%** (-6%, +30%)
Extreme Statistics	2-yr	**+25%** (+5%, +55%)	**+25%** (+10%, +42%)	**+15%** (-10%, +42%)	**-2%** (-31%, +54%)	**+30%** (-2%, +55%)
	5-yr	**+29%** (+1%, +77%)	**+27%** (+7%, +49%)	**+17%** (-11%, +66%)	**+4%** (-28%, +87%)	**+38%** (-3%, +83%)
	10-yr	**+32%** (-1%, +94%)	**+28%** (+6%, +60%)	**+18%** (-14%, +77%)	**+8%** (-30%, +110%)	**+44%** (-3%, +107%)
	25-yr	**+37%** (-6%, +117%)	**+30%** (+5%, +75%)	**+20%** (-15%, +87%)	**+14%** (-34%, +142%)	**+54%** (-2%, +145%)
	50-yr	**+42%** (-13%, +136%)	**+32%** (+3%, +87%)	**+21%** (-15%, +92%)	**+20%** (-37%, +167%)	**+63%** (-1%, +180%)
	100-yr	**+48%** (-19%, +157%)	**+34%** (+1%, +100%)	**+23%** (-22%, +110%)	**+27%** (-39%, +195%)	**+73%** (-3%, +221%)

Table 2. Projected changes (%) in 1-hour precipitation statistics for the WRF grid point closest to Portland Airport, for the 2080s (2070-2099) relative to 1981-2010. The table shows the changes for 12 WRF projections (average, minimum, and maximum), all based on a high-end greenhouse gas scenario (RCP 8.5). Columns show results for the full water year (Oct-Sep), as well as for winter (Dec-Feb), spring (Mar-May), summer (Jun-Aug), and fall (Sep-Dec). Rows show the projected change in the total precipitation for each time period as well as the extreme statistics corresponding to the 2-, 5-, 10-, 25-, 50-, and 100-year events.

water year, followed by the statistics for each season starting in winter (Dec-Feb) and ending in fall (Sep-Nov).

The percent change in total precipitation is included for comparison with the extreme statistics: models generally show much smaller changes in seasonal and annual totals, whereas changes are larger for the extreme statistics. Focusing on the 10-year event (10% annual chance of exceedance) and the 1-hour duration, Table 5 shows a projected change of +32% (range: -1% to +94%) when considering the full water year. Projected changes are smaller for spring, especially summer, and larger for fall. Overall, the projections show consistent increases across nearly all return intervals and seasons, with very few models

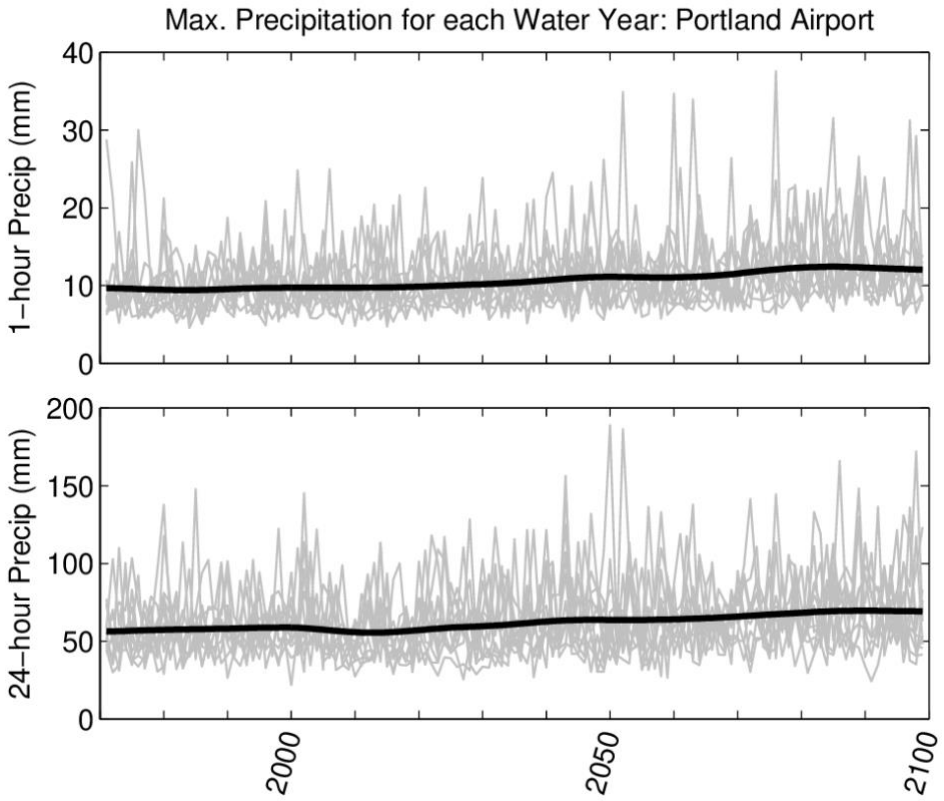

Figure 7. Time series of the water year maximum in 1-hour (top) and 24-hour (bottom) precipitation for the grid cell closest to Portland Airport. Results are shown for all 12 RCP 8.5 WRF projections (light grey lines), and for the average among all models for each water year (thick black line). To simplify interpretation, the model average is smoothed using a 31-point Gaussian filter.

showing decreases and when they do these are fairly modest. The one exception is summer, where the smaller events (2-yr, 5-yr) show an average change that is near zero, with about an equal number of models showing decreases as increases. Another notable aspect of summer precipitation is that the seasonal total is projected to decrease, whereas the models tend to show increases in the intensity of the big events. Finally, there is a tendency for the largest events to show the largest increases in intensity (e.g., the average change for the 5-year is greater than for the 2-year event). This result should be treated with caution, given that the projected changes are calculated from 30-year samples, which makes it difficult to accurately estimate the magnitude of the larger extremes (e.g., 50-year, 100-year events).

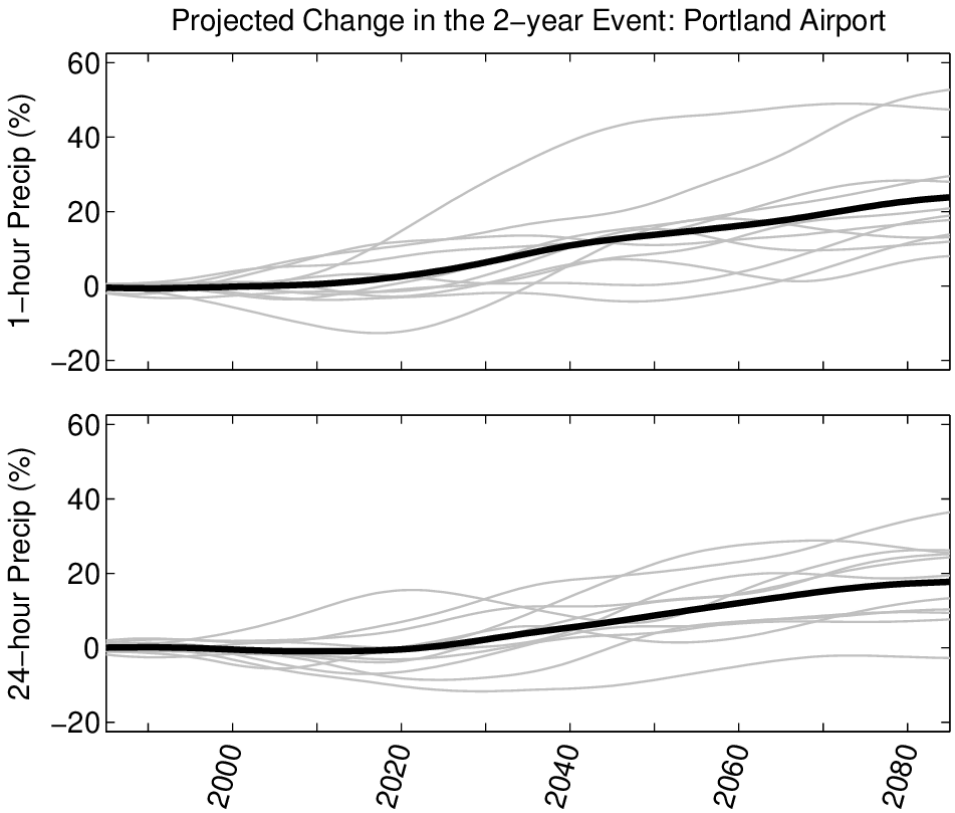

Figure 8. As in Figure 7, except showing the percent change, relative to 1981-2010, in the 2-year precipitation extreme for the 1-hour (top) and 24-hour durations (bottom). In order to simplify interpretation, each model projection was smoothed using a 31-point Gaussian filter.

Figure 7 shows the time series of the annual maximum precipitation at the Portland Airport (NOAA-LCD, station ID: 72698024229), for 1-hour and 24-hour durations, for each water year. Since we are showing the precipitation amounts, in mm, we used the results that have been bias-corrected to match the observations at this site. Consistent with Table 5, these show a clear tendency towards larger events. Given the limitations of bias-correction, our recommendation is to use the percent change in precipitation extremes whenever possible. We nonetheless include Figure 7 to illustrate the intermittency in extreme precipitation events. This is shown clearly in the plot: Although the average line shows a long-term tilting of the odds towards larger events, the exact timing of the largest events is somewhat random, making it hard to discern trends over time.

Figure 8 shows the percent change in the 2-year precipitation event, as computed in the visualization described above. Since we are showing the percent change, these results are based on the raw (i.e.: not bias-corrected) WRF projections. In order to focus on the long-term change, the results are also smoothed with a 31-year gaussian filter, which closely matches the 30-year time periods used to calculate the 2-year precipitation statistic. These show a clear trend over time in the model average, with substantial variability among the 12 model projections. Both the

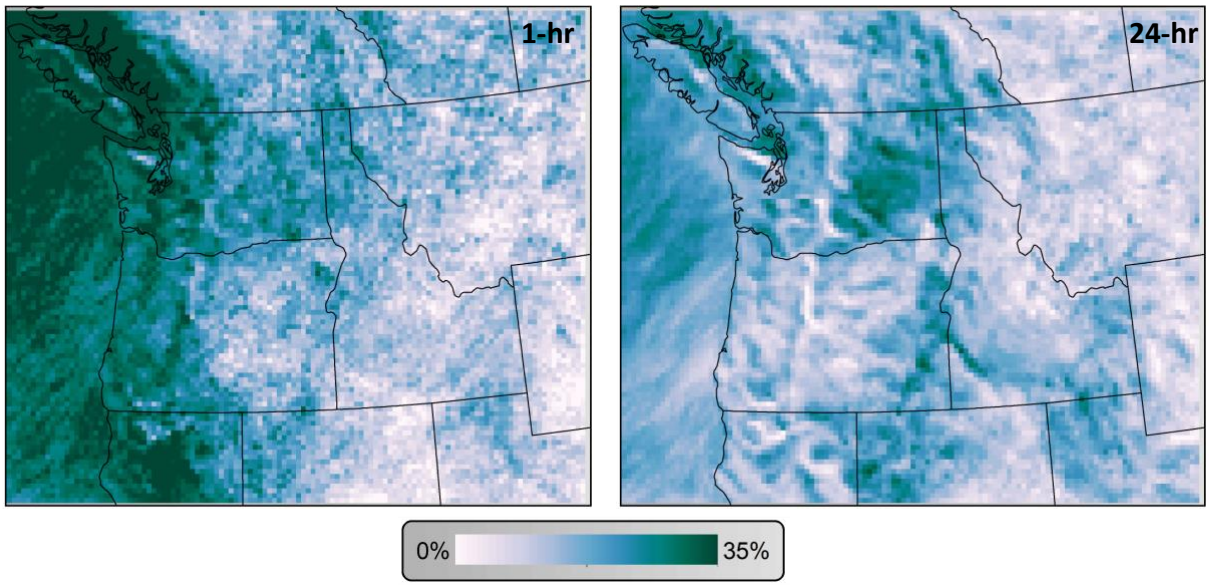

Figure 9. Average projected change in the 2-year, for 1-hr (left) and 24-hour (right) durations, for the full WRF model domain. Changes are shown for the 2080s (2070-2099) relative to 1981-2010.

projected change, and the range among models, is greater for the 1-hour than for the 24-hour duration.

The above projections, though representative of the region, only show results for the grid cell closest to Portland Airport. In order to see how these changes vary across the region, Figure 9 shows the projected change in the 2-year event for the 2080s (2070-2099), for the full WRF model domain. As with Portland Airport, these show that the projected changes for the 1-hour event are greater than those for the 24-hour event. The maps also show larger changes west of the Cascades, whereas changes east of the Cascades are generally less pronounced. The pixilation in the maps suggests that there is considerable noise associated with estimating changes in extreme statistics. Future work will consider how to extract more robust trends from these projections.

Considerations for Interpreting the Results

A number of considerations may be helpful to keep in mind when reviewing the projections:

- Projected changes will always be governed by a combination of natural variability and long-term trends due to climate change. This is particularly true for changes in extremes: Since, by definition, these events are rare, it is difficult to accurately assess how rapidly they will change. Although the 2080s projections can be significantly influenced by natural variability, we recommend focusing on these late-century projections since this is when the projected changes will be largest relative to natural variability.
- The extremes estimates are limited by sample size. Whereas the 2- and 5-year events are relatively well captured in a 30-year record (e.g., 1970-1999, 2070-2099), extrapolation is needed to estimate the 50- and 100-year extremes. This means that the 50- and 100-year estimates are more prone to noise. For example, if the simulation includes one particularly large storm in the historical record, this could artificially mute the projected change estimates even if, on average, most storms do become more intense. The converse is also true: a large storm at the end of the 21st century could artificially inflate the projected change.
- Projected changes differ substantially for different precipitation durations. In general, changes appear to be largest for 1-hour precipitation and smallest for the longest durations. This is consistent with previous research projecting a change in atmospheric river events yet very little change in seasonal or annual precipitation.

- The WRF model used in this study has a spatial resolution of 12 km. This is not enough to explicitly resolve convective precipitation, such as thunderstorms. Although these are represented statistically by the model, researchers generally consider that a finer resolution is needed to accurately capture convective events. This means that the current projections should be viewed primarily as an estimate of the change in the intensity of large-scale heavy precipitation events such as atmospheric rivers. Since thunderstorms are most prevalent in summer, predominantly east of the Cascades, this limitation in the WRF model is most likely to affect projected changes in summer precipitation events east of the Cascade Range.
- We estimated extremes by fitting a GEV distribution with L-moments (Section 6). This approach will result in different estimates than the standard (e.g., Bulletin 17B, 1982) methods that are prescribed in certain applications. In most cases, these differences should be minor. We note this only because some applications require the use of the Bulletin 17B approach.

Future Work

A primary challenge in this work is that it is difficult to detect changes in the frequency of rare events. This could be addressed through new approaches for detecting trends. For example, bootstrap approaches can be used to minimize the effect of outliers (e.g., Byun and Hamlet, 2020). There is considerable literature on the topic of trends in extremes; future work could explore approaches for developing more robust trend estimates.

There are two other issues that merit further study: (1) regionalized precipitation statistics, and (2) optimizing the WRF model configuration.

Another potential advancement would be to "regionalize" the extreme precipitation statistics by assuming that extremes across select areas follow a similar distribution. This improves the reliability of extremes estimates, particularly for gauges with short records. This information could also be used to further improve the bias correction approach.

Additional work also could be done to optimize the WRF model configuration. This effort could be scaled depending on the time and resources that are available; the focus would be to compare the performance of the WRF model for different spatial resolutions and parameterizations affecting precipitation formation. For example, the current resolution of 12

km does not appear adequate for capturing convective precipitation events, such as thunderstorms.

Finally, in the current project we were able to analyze results for the entire WRF model domain, providing percent changes in precipitation across the Pacific Northwest. This could be further expanded by obtaining additional rain gauge observations from across the region, many of which are managed by specific jurisdictions and not always publicly available. In addition, many regulatory contexts and design tools require data to be processed and packaged in a particular way. Additional work could be done to facilitate the use and application of the results in these contexts.

References

Abatzoglou, J. T., & Brown, T. J. (2012). A comparison of statistical downscaling methods suited for wildfire applications. *International Journal of Climatology*, *32*(5), 772-780. https://doi.org/10.1002/joc.2312

Brekke, L. D., Dettinger, M. D., Maurer, E. P., & Anderson, M. (2008). Significance of model credibility in estimating climate projection distributions for regional hydroclimatological risk assessments. *Climatic Change*, *89*(3-4), 371-394. http://dx.doi.org/10.1007/s10584-007-9388-3

Brewer, M. C., & Mass, C. F. (2016). Projected changes in western US large-scale summer synoptic circulations and variability in CMIP5 models. *Journal of Climate*, *29*(16), 5965-5978. https://doi.org/10.1175/JCLI-D-15-0598.1

Byun, K., & Hamlet, A. F. (2020). A risk-based analytical framework for quantifying non-stationary flood risks and establishing infrastructure design standards in a changing environment. Journal of Hydrology, 584, 124575. https://doi.org/10.1016/j.jhydrol.2020.124575

Dulière, V., Zhang, Y., & Salathé Jr, E. P. (2011). Extreme precipitation and temperature over the US Pacific Northwest: A comparison between observations, reanalysis data, and regional models. Journal of Climate, 24(7), 1950-1964. https://doi.org/10.1175/2010JCLI3224.1

Flato, G., Marotzke, J., Abiodun, B., Braconnot, P., Chou, S. C., Collins, W., ... & Rummukainen, M. (2014). Evaluation of climate models. In Climate change 2013: the physical science basis. Contribution of Working Group I to the Fifth Assessment Report of the Intergovernmental Panel on Climate Change (pp. 741-866). Cambridge University Press. https://www.ipcc.ch/site/assets/uploads/2018/02/WG1AR5_Chapter09_FINAL.pdf

Hosking, J. R. M., & Wallis, J. R. (2005). Regional frequency analysis: an approach based on L-moments. Cambridge university press.

Lorente-Plazas, R., Mitchell, T. P., Mauger, G., & Salathé Jr, E. P. (2018). Local enhancement of extreme precipitation during atmospheric rivers as simulated in a regional climate model. Journal of Hydrometeorology, 19(9), 1429-1446. https://doi.org/10.1175/JHM-D-17-0246.1

Mauger, G.S., J.S. Won, K. Hegewisch, C. Lynch, R. Lorente Plazas, E. P. Salathé Jr., 2018. New Projections of Changing Heavy Precipitation in King County. Report prepared for the

King County Department of Natural Resources. Climate Impacts Group, University of Washington, Seattle. https://cig.uw.edu/publications/new-projections-of-changing-heavy-precipitation-in-king-county-2/

Mauger, G.S., S.-Y. Lee, C. Bandaragoda, Y. Serra, J.S. Won, (2016). Refined Estimates of Climate Change Affected Hydrology in the Chehalis basin. Report prepared for Anchor QEA, LLC. Climate Impacts Group, University of Washington, Seattle. https://doi.org/10.7915/CIG53F4MH

Mauger, G.S., J.H. Casola, H.A. Morgan, R.L. Strauch, B. Jones, B. Curry, T.M. Busch Isaksen, L. Whitely Binder, M.B. Krosby, and A.K. Snover. 2015. *State of Knowledge: Climate Change in Puget Sound.* Report prepared for the Puget Sound Partnership and the National Oceanic and Atmospheric Administration. Climate Impacts Group, University of Washington, Seattle. https://dx.doi.org/10.7915/CIG93777D

Millington, N., Das, S., & Simonovic, S. P. (2011). The comparison of GEV, log-Pearson type 3 and Gumbel distributions in the Upper Thames River watershed under global climate models. https://ir.lib.uwo.ca/wrrr/40/

Rahman, A., Karin, F., & Rahman, A. (2015, November). Sampling variability in flood frequency analysis: How important is it. In 21st International Congress on Modelling and Simulation, Gold Coast, Australia (pp. 2200-2206). https://www.researchgate.net/profile/Ayesha_Rahman3/publication/311438936_Sampling_Variability_in_Flood_Frequency_Analysis_How_Important_is_it/links/58466a0308ae61f75dd9689b/Sampling-Variability-in-Flood-Frequency-Analysis-How-Important-is-it

Rahman, A., Weinmann, P. E., & Mein, R. G. (1999). At-site flood frequency analysis: LP3-product moment, GEV-L moment and GEV-LH moment procedures compared. In Water 99: Joint Congress; 25th Hydrology & Water Resources Symposium, 2nd International Conference on Water Resources & Environment Research; Handbook and Proceedings (p. 715). Institution of Engineers, Australia.

Rupp, D. E., Abatzoglou, J. T., Hegewisch, K. C., & Mote, P. W. (2013). Evaluation of CMIP5 20th century climate simulations for the Pacific Northwest USA. Journal of Geophysical Research: Atmospheres, 118(19), 10-884. https://doi.org/10.1002/jgrd.50843

Salathé Jr., Eric P., Alan F. Hamlet, Clifford F. Mass, Se-Yeun Lee, Matt Stumbaugh, and Richard Steed, 2014: Estimates of Twenty-First-Century Flood Risk in the Pacific Northwest Based

on Regional Climate Model Simulations. J. Hydrometeor, 15, 1881–1899. http://dx.doi.org/10.1175/JHM-D-13-0137.1

Salathé, E. P., Leung, L. R., Qian, Y., & Zhang, Y. (2010). Regional climate model projections for the State of Washington. *Climatic Change*, *102*(1-2), 51-75. https://link.springer.com/content/pdf/10.1007/s10584-010-9849-y.pdf

Skamarock, W. C., Klemp, J. B., Dudhia, J., Gill, D. O., Barker, D. M., Wang, W., & Powers, J. G. (2005). A description of the advanced research WRF version 2 (No. NCAR/TN-468+ STR). National Center For Atmospheric Research Boulder Co Mesoscale and Microscale Meteorology Div.

Taylor, K. E., Stouffer, R. J., & Meehl, G. A. (2012). An overview of CMIP5 and the experiment design. *Bulletin of the American Meteorological Society*, *93*(4), 485-498. https://doi.org/10.1175/BAMS-D-11-00094.1

Tohver, I. M., Hamlet, A. F., & Lee, S. Y. (2014). Impacts of 21st-century climate change on hydrologic extremes in the Pacific Northwest region of North America. JAWRA Journal of the American Water Resources Association, 50(6), 1461-1476. https://doi.org/10.1111/jawr.12199

Trenberth, K. E. (2011). Changes in precipitation with climate change. *Climate Research*, *47*(1-2), 123-138. https://doi.org/10.3354/cr00953

Van Vuuren, D., J. Edmonds, M. Kainuma, K. Riahi, A. Thomson, K. Hibbard, G. Hurtt, T. Kram, V. Krey, J. Lamarque, T. Masui, M. Meinshausen, N. Nakicenovic, S. Smith, S. Rose, 2011: The representative concentration pathways: an overview. *Climatic Change*, **109**: 5-31. http://dx.doi.org/10.1007/s10584-011-0148-z

Vogel, R. M., McMahon, T. A., & Chiew, F. H. (1993). Floodflow frequency model selection in Australia. Journal of Hydrology, 146, 421-449. https://doi.org/10.1016/0022-1694(93)90288-K

Warner, M. D., Mass, C. F., & Salathé Jr, E. P. (2015). Changes in winter atmospheric rivers along the North American west coast in CMIP5 climate models. *Journal of Hydrometeorology*, *16*(1), 118-128. https://doi.org/10.1175/JHM-D-14-0080.1

Wuertz, D., Lawrimore, J., and Korzeniewski, B. (2018). Cooperative Observer Program (COOP) Hourly Precipitation Data (HPD), Version 2.0. NOAA National Centers for Environmental Information. doi:10.25921/p7j8-2170. *Accessed on 17 Aug 2020*.

Appendix

Table A1. All rain gauge stations used in the analysis. For the HYDRA and HPD networks, the stations with less than 10 effective years of data were excluded from the analysis. "Effective years" is defined as the number of years for which >90% of data are valid for all months of the year.

Network	ID	Name	Lat. / Lon.	Years
NOAA HPD	USC00350126	Allegany	43.42910N / 124.03050W	1953-1995
NOAA HPD	USC00350265	Arlington	45.72120N / 120.20640W	1951-2020
NOAA HPD	USC00350356	Auston	44.57470N / 118.49130W	1980-2016
NOAA HPD	USC00350471	Bandon	43.14970N / 124.40190W	1949-2020
NOAA HPD	USC00350571	Bear Springs Rs	45.12670N / 121.53440W	1963-2011
NOAA HPD	USC00350694	Bend	44.05690N / 121.28500W	1950-1999
NOAA HPD	USC00350781	Black Butte	43.59470N / 123.07050W	1950-2020
NOAA HPD	USC00450729	Blaine	48.97750N / 122.79270W	1953-2007
NOAA HPD	USC00350853	Bly RS	42.40000N / 121.04580W	1954-2018
NOAA HPD	USC00351033	Brightwood	45.38530N / 122.04580W	1975-2020
NOAA HPD	USC00351149	Buncom	42.18000N / 122.98520W	1949-2015
NOAA HPD	USC00450986	Burlington 5N	48.55000N / 122.33330W	1956-2018
NOAA HPD	USC00351222	Buxton	45.68980N / 123.19060W	1950-2018
NOAA HPD	USC00451160	Carson FH	45.86770N / 121.97330W	1979-2020
NOAA HPD	USC00351433	Cascadia	44.39130N / 122.48110W	1950-2006
NOAA HPD	USC00451400	Chief Joseph Dam	47.99670N / 119.64820W	1953-2015
NOAA HPD	USC00351643	Clatskanie	46.10810N / 123.20580W	1955-2020
NOAA HPD	USC00351735	Colton	45.17280N / 122.43420W	1952-2020
NOAA HPD	USC00351765	Condon	45.24080N / 120.17900W	1953-2013
NOAA HPD	USC00351902	Cottage Grove Dam	43.71780N / 123.05780W	1949-2020
NOAA HPD	USC00451759	Cougar	46.00860N / 122.34550W	1951-2020
NOAA HPD	USC00351914	Cougar Dam	44.13080N / 122.24190W	1961-2020
NOAA HPD	USC00452030	Dayton	46.31520N / 118.00220W	1978-2020
NOAA HPD	USC00352292	Detroit Dam	44.72410N / 122.25470W	1957-2020
NOAA HPD	USC00352295	Devils Flat	42.81220N / 123.04560W	1978-2018
NOAA HPD	USC00352345	Disston	43.70770N / 122.73940W	1957-2017
NOAA HPD	USC00352374	Dorena	43.78220N / 122.96300W	1952-2020
NOAA HPD	USC00352408	Drain	43.78450N / 123.42470W	1958-2019
NOAA HPD	USC00452384	Easton	47.24220N / 121.18690W	1949-2012
NOAA HPD	USC00452505	Ellensburg	47.00000N / 120.51670W	1955-1996
NOAA HPD	USC00352697	Estacada	45.07670N / 121.97140W	1949-2020
NOAA HPD	USC00352867	Fern Ridge - Veneta	44.04940N / 123.37020W	1949-2020
NOAA HPD	USC00352972	Florence	44.00000N / 124.11670W	1955-2020
NOAA HPD	USC00353047	Foster Dam	44.41390N / 122.67280W	1970-2020
NOAA HPD	USC00353232	Gerber Dam	42.20520N / 121.13140W	1976-2020
NOAA HPD	USC00353305	Glendale	42.76670N / 123.40000W	1955-2020
NOAA HPD	USC00353318	Glenwood	45.65610N / 123.31080W	1960-2020
NOAA HPD	USC00453183	Glenwood	46.00800N / 121.26230W	1956-2017

NOAA HPD	USC00353340	Goble	45.98980N / 122.92560W	1949-2020
NOAA HPD	USC00353402	Government Camp	45.30080N / 121.74250W	1967-2020
NOAA HPD	USC00353604	Halfway	44.87730N / 117.10950W	1976-2014
NOAA HPD	USC00453515	Harrington	47.48290N / 118.25190W	1962-2017
NOAA HPD	USC00353915	Hills Cr Dam	43.75000N / 122.50000W	1963-2020
NOAA HPD	USC00354238	Jefferson	44.72340N / 123.01340W	1949-2020
NOAA HPD	USC00354321	Jordan Valley	42.97920N / 117.05330W	1950-2009
NOAA HPD	USC00354622	LaGrande	45.31670N / 118.07470W	1968-2008
NOAA HPD	USC00454679	Lind	47.00220N / 118.56570W	1950-2018
NOAA HPD	USC00355050	Lookout Point Dam	43.91390N / 122.76000W	1956-2020
NOAA HPD	USC00355213	Marcola	44.17060N / 122.87140W	1953-2020
NOAA HPD	USC00355221	Marion FFH	44.61250N / 121.94860W	1959-2019
NOAA HPD	USC00455549	Montesano	47.01670N / 123.65000W	1955-2017
NOAA HPD	USC00355734	Moro	45.48250N / 120.72360W	1950-2002
NOAA HPD	USC00455731	Naches	46.86670N / 120.77470W	1956-2015
NOAA HPD	USC00355969	Newhalem	45.71490N / 123.88690W	1949-2019
NOAA HPD	USC00455946	Northport	48.89940N / 117.82900W	1962-2014
NOAA HPD	USC00356238	Ochoco Dam	44.29940N / 120.72640W	1953-2000
NOAA HPD	USC00456789	Pullman	46.76020N / 117.18610W	1950-2016
NOAA HPD	USC00456851	Quilcene Dam	47.78470N / 122.97970W	1950-2009
NOAA HPD	USC00456864	Quinault RS	47.50000N / 123.81670W	1979-2016
NOAA HPD	USC00456982	Republic RS	48.65010N / 118.73250W	1952-2018
NOAA HPD	USC00357127	Rex	45.30330N / 122.91330W	1952-2020
NOAA HPD	USC00357554	Santiam Junct	44.43550N / 121.94280W	1962-2020
NOAA HPD	USC00357572	Sauvies Island	45.65550N / 122.83380W	1952-2020
NOAA HPD	USC00357817	Silver Lake RS	43.12470N / 121.06150W	1985-2017
NOAA HPD	USC00357823	Silverton	45.00580N / 122.77390W	1963-2020
NOAA HPD	USC00458207	Sunnyside	46.32360N / 120.01030W	1951-1996
NOAA HPD	USC00358263	Sutherlin	43.46670N / 123.06670W	1956-2014
NOAA HPD	USC00358504	Tillamook	45.46670N / 123.66670W	1949-2016
NOAA HPD	USC00358512	Tiller	43.00670N / 122.69610W	1957-2015
NOAA HPD	USC00358717	Tygh Valley	45.24610N / 121.17110W	1975-2020
NOAA HPD	USC00358790	Upper Steamboat Cr	43.48250N / 122.60080W	1959-2002
NOAA HPD	USC00358884	Vernonia	45.86520N / 123.19020W	1973-2020
NOAA HPD	USC00359213	Weston	45.82140N / 118.43030W	1957-2019
NOAA HPD	USC00459200	Whitman Mission	46.04360N / 118.46280W	1964-2020
NOAA HPD	USC00359581	Yaquina Bay Lightboat	44.63330N / 124.05000W	1970-2020
NOAA LCD	72791094224	Astoria Airpt	46.15690N / 123.88250W	1973-2020
NOAA LCD	72693024221	Eugene Mahlon Sweet Fld	44.12458N / 123.21197W	1973-2020
NOAA LCD	72597024225	Medford Airpt	42.38110N / 122.87220W	1973-2020
NOAA LCD	72792024227	Olympia Airpt	46.97330N / 122.90330W	1973-2020
NOAA LCD	72698024229	Portland Airpt	45.59083N / 122.60028W	1936-2020
NOAA LCD	72797094240	Quillayute Airpt	47.93658N / 124.56263W	1973-2020
NOAA LCD	72694024232	Salem Airpt McNary Fld	44.90953N / 123.00250W	1973-2020
NOAA LCD	72793024233	Sea-Tac Airpt	47.44469N / 122.31437W	1948-2020

NOAA LCD	72785024157	Spokane Airpt	47.62160N / 117.52800W	1941-2020
NOAA LCD	72781024243	Yakima Airpt	46.56817N / 120.54406W	1973-2020
HYDRA	111	Airport Way PS02	45.55884N / 122.51288W	2000-2019
HYDRA	117	AlbinaPS	45.54082N/122.67758W	2001-2019
HYDRA	1	Ankeny FS	45.52210N / 122.67061W	1996-2019
HYDRA	174	Arleta School	45.48620N / 122.59592W	2004-2019
HYDRA	193	Astor School	45.57891N / 122.72971W	2007-2019
HYDRA	152	Beaumont School	45.54869N / 122.62133W	1997-2019
HYDRA	58	Bonny Slope School	45.54546N / 122.78368W	1980-2015
HYDRA	153	Cascade PCC	45.56358N / 122.67352W	1977-2019
HYDRA	192	Childrens Museum	45.50856N / 122.71787W	2007-2018
HYDRA	10	Collins View	45.45410N / 122.68434W	1977-2019
HYDRA	107	Columbial PS	45.59481N / 122.71731W	1977-2018
HYDRA	144	Columbia STP	45.59479N / 122.71732W	1977-2018
HYDRA	146	Cottrell School	45.45377N / 122.28849W	1989-2019
HYDRA	12	Fernwood	45.53676N / 122.63152W	1979-2011
HYDRA	012F	Fernwood	45.53676N / 122.63152W	1977-2011
HYDRA	72	Fremont PS	45.54217N / 122.57131W	1982-2010
HYDRA	317	Fremont PS	45.54216N / 122.57133W	1982-2010
HYDRA	175	Glencoe ES	45.51682N / 122.61115W	2003-2018
HYDRA	20	Gresham Fire	45.50758N / 122.43732W	1991-2019
HYDRA	125	Guilds PS	45.57305N / 122.75041W	1977-2004
HYDRA	64	Harney PS	45.46229N / 122.64320W	1992-2019
HYDRA	7	Hayden Island PS	45.61202N / 122.68867W	1995-2018
HYDRA	21	Holgate PS	45.48953N / 122.52443W	1992-2012
HYDRA	14	Kelly School	45.47292N / 122.57005W	1979-2019
HYDRA	014F	Kelly School	45.47292N / 122.57005W	1977-2019
HYDRA	130	Linnton PS	45.60060N / 122.78563W	1979-1999
HYDRA	213	Madison HS	45.54333N / 122.58078W	2010-2019
HYDRA	115	Mallory PS	45.58146N / 122.66311W	1996-2019
HYDRA	172	Maplewood ES	45.47066N / 122.73023W	2003-2019
HYDRA	137	Marine Dr PS	45.62796N / 122.74150W	1985-2010
HYDRA	173	Metro Learning Ctr	45.52681N / 122.69324W	2003-2019
HYDRA	6	Mt Tabor Yard	45.50574N / 122.59662W	1977-2018
HYDRA	181	Multnomah Co	45.51270N / 122.66013W	2005-2019
HYDRA	48	Open Meadows	45.57799N / 122.69961W	1996-2018
HYDRA	9	PDX Bus Park PS	45.57260N / 122.57378W	1992-2003
HYDRA	159	PDX Post Office PS	45.58389N / 122.58293W	2005-2019
HYDRA	145	Pleasant Valley	45.46475N / 122.47963W	1977-2019
HYDRA	3	Sauvies Island School	45.65530N / 122.82528W	1978-2011
HYDRA	147	Skyline FS	45.59393N / 122.81848W	1977-2002
HYDRA	2	Skyline School	45.60784N / 122.85665W	1977-2019
HYDRA	171	Sunnyside School	45.51458N / 122.62925W	2004-2019
HYDRA	164	SW 12th And Clay	45.51517N / 122.68753W	2001-2019
HYDRA	204	Swan Island CSO PS	45.55337N / 122.69606W	2008-2019

HYDRA	122	Swan Island PS	45.55527N / 122.69313W	1995-2007
HYDRA	4	Sylvania PCC	45.43685N / 122.73175W	1977-2019
HYDRA	161	Sylvan School	45.50994N / 122.73700W	2001-2017
HYDRA	167	Terminal 4	45.60076N / 122.77156W	2001-2011
HYDRA	120	Thomas PS	45.49392N / 122.67270W	1996-2009
HYDRA	89	Vermont Hills	45.47704N / 122.73618W	1985-2001
HYDRA	41	Vernon School	45.56243N / 122.64343W	1996-2018
HYDRA	300	West TV School	45.51528N / 122.76712W	1977-1995
HYDRA	160	WPCL	45.58569N / 122.75947W	2001-2019
HYDRA	121	Yeon PS	45.54618N / 122.71031W	1986-2019
Everett	FS4	Fire Station 4	47.94398N / 122.24303W	2012-2017
Everett	FS6	Fire Station 6	47.91212N / 122.23868W	2012-2017
Everett	LgnGolf	Legion Golf Course	48.01072N / 122.20142W	2012-2014
Everett	LS2	Lift Station 2	47.97769N / 122.22118W	2012-2017
Everett	LS33	Lift Station 33	47.96999N / 122.19012W	2012-2017
Everett	LS8	Lift Station 8	47.99909N / 122.21274W	2012-2017
Everett	LS9	Lift Station 9	47.99524N / 122.18375W	2012-2017
Everett	NCrk124	North Cr 124	47.88533N / 122.22363W	2014-2017
Everett	SrvCtrEvt	Service Center	47.97530N / 122.19503W	2014-2017
KingCty	BART	Barton	47.53276N / 122.37478W	2013-2017
KingCty	XRDS	Bellevue Crossroads I&I	47.61734N / 122.12562W	2001-2017
KingCty	BDIA	Black Diamond I&I	47.30523N / 122.00601W	2001-2017
KingCty	02v	Blakely Ridge	47.71857N / 122.04295W	1990-2013
KingCty	04u	Boeing Cr	47.74965N / 122.35963W	1990-2017
KingCty	BOTH	Bothell I&I	47.79104N / 122.23285W	2002-2017
KingCty	BC-Rain	Boulder Cr Apts	47.56589N / 122.02631W	2010-2017
KingCty	BW-rain	Brightwater	47.79171N / 122.14292W	2006-2017
KingCty	35u	Bruggers Bog	47.77198N / 122.30305W	1992-2017
KingCty	05u	Cherry Cr	47.74258N / 121.90845W	2009-2017
KingCty	CL-MET	Cold Creek	47.74987N / 122.09711W	2007-2009
KingCty	02w	Cottage Lk	47.75758N / 122.08026W	1993-2017
KingCty	63y	Cougar Mt	47.54110N / 122.09838W	1997-2017
KingCty	09V	Covington Cr	47.32160N / 122.04125W	2005-2017
KingCty	11u	Des Moines Cr	47.42708N / 122.30621W	1992-2017
KingCty	24v	East Fork Hylebos	47.26284N / 122.31267W	1997-2017
KingCty	14u	East Fork Issaquah	47.53170N / 121.98718W	1988-2017
KingCty	36V	East Maury Island	47.38630N / 122.37609W	2011-2017
KingCty	44u	Enumclaw	47.20740N / 121.95570W	1999-2017
KingCty	FACT	Factoria I&I	47.58314N / 122.15806W	2002-2017
KingCty	31Y2	Fairwood	47.44325N / 122.14350W	2010-2017
KingCty	hau	Hamm Creek	47.51488N / 122.30945W	1996-2014
KingCty	31z	Hobart	47.41681N / 121.94282W	1995-2017
KingCty	51w	Hollywood Hill	47.72625N / 122.12411W	1988-2017
KingCty	26u	Jenkins Cr	47.35956N / 122.06755W	1992-2017
KingCty	GAFEN2	Juanita Creek	47.73061N / 122.17117W	1988-2019

KingCty	KANG	Kent Kangley I&I	47.35785N / 122.13277W	2001-2017
KingCty	KIRK	Kirkland I&I	47.68230N / 122.19228W	2001-2017
KingCty	SKY1	Lakeridge Elem School	47.50039N / 122.24068W	2004-2013
KingCty	SERE	Lake Serene I&I	47.87185N / 122.29195W	2001-2017
KingCty	LHPS	Lakland Hills	47.26995N / 122.22085W	2001-2017
KingCty	BEAR	Little Bear I&I	47.79037N / 122.13289W	2001-2017
KingCty	41v	Lk Dolloff	47.32145N / 122.29200W	1989-2017
KingCty	42u	Lk Reba	47.46666N / 122.31327W	1991-2017
KingCty	32u	Lower Green R	47.31956N / 122.17971W	1989-2017
KingCty	37u	Lower May Cr	47.51235N / 122.14882W	1991-2017
KingCty	MCSN	Martha Lake I&I	47.85867N / 122.23930W	2002-2017
KingCty	MARY	Marymoor Park I&I	47.66354N / 122.12015W	2004-2017
KingCty	36U	Maury Island	47.39959N / 122.43448W	2005-2017
KingCty	25v	McDonald Cr	47.47884N / 122.05988W	1988-2017
KingCty	MERC	Mercer Island I&I	47.57218N / 122.22380W	2001-2017
KingCty	40u	Middle Green	47.26070N / 122.09187W	1992-2017
KingCty	18Y	Mystic Lk	47.62790N / 122.02493W	2001-2017
KingCty	MNCR	North Creek Maltby I&I	47.81789N / 122.19762W	2001-2017
KingCty	43u	North Vashon	47.48771N / 122.46985W	1999-2017
KingCty	51u	Norway	47.74167N / 122.20983W	1988-2017
KingCty	NOVH	Novelty Hill I&I	47.69184N / 122.08887W	2001-2017
KingCty	03u	Panther Cr	47.41557N / 122.20032W	1989-2017
KingCty	48Y	Patterson Cr Upper	47.63892N / 122.00776W	2003-2017
KingCty	18V2	Redmond Ridge	47.67940N / 122.03476W	2011-2017
KingCty	31UN	Renton Roads	47.48189N / 122.17426W	2001-2017
KingCty	SAHA	Sahale I&I	47.64949N / 122.04403W	2001-2017
KingCty	50u	Salmon Cr	47.50197N / 122.35185W	1992-2017
KingCty	SAMP	Sammamish Pleateau I&I	47.58047N / 122.02526W	2001-2017
KingCty	51T	Sammamish R	47.70302N / 122.14366W	2006-2017
KingCty	SEQU	Sequioia Jr HS I&I	47.36701N / 122.19304W	2001-2017
KingCty	54v	Soos Cr	47.37961N / 122.14360W	1992-2017
KingCty	41u	Star Lk	47.35259N / 122.28914W	1989-2017
KingCty	65U	Tahlequah	47.35050N / 122.51111W	2005-2017
KingCty	67u	Tibbetts Creek	47.52670N / 122.06297W	1988-2017
KingCty	Trilogy-met	Triology Golf Course	47.69998N / 122.02790W	2006-2017
KingCty	02VN	Triology North	47.71939N / 122.02765W	2014-2017
KingCty	TUKW	Tukwila I&I	47.44845N / 122.25478W	2001-2017
KingCty	19U	Twin Cedars	47.56529N / 121.89455W	2010-2017
KingCty	37W	Upper Ma yCr	47.49867N / 122.09275W	2001-2016
KingCty	28Y	West Judd Cr	47.43699N / 122.49933W	2005-2017
Seattle	rg07	15th Ave NW	47.69712N / 122.37819W	1976-2016
Seattle	rg12	34th Ave W	47.64309N / 122.40042W	1976-2016
Seattle	rg10	Beacon Ave S	47.49830N / 122.26344W	1976-2016
Seattle	rg11	Denn ySt	47.61861N / 122.35975W	1976-2016
Seattle	rg15	Diagonal Ave S	47.56231N / 122.33996W	1976-2016

Seattle	rg16	East Marginal Wy S	47.53666N / 122.31812W	1976-2016
Seattle	rg20	E Union St	47.61307N / 122.30955W	1976-2016
Seattle	rg05	Fauntleroy Ferry	47.52331N / 122.39397W	1976-2016
Seattle	rg25	Garfield Comm Ctn	47.60786N / 122.30215W	2017-2019
Seattle	rg08	Gov tLocks	47.66544N / 122.39590W	1976-2016
Seattle	rg01	N 128th St	47.72188N / 122.33946W	1976-2016
Seattle	rg04	NE 86th St	47.69077N / 122.31815W	1976-2016
Seattle	rg02	NE 93rd St	47.69629N / 122.27314W	1976-2016
Seattle	rg03	NE Pacific St	47.64962N / 122.30881W	1976-2016
Seattle	rg18	Rainier Ave S	47.54961N / 122.27714W	1976-2016
Seattle	rg30	Rainier Beach Public Lib	47.52154N / 122.27054W	2017-2019
Seattle	rg17	SW Barton St	47.52092N / 122.34518W	1976-2016
Seattle	rg14	Walnut Ave W	47.57603N / 122.38419W	1976-2016
Seattle	rg09	Woodland Park Zoo	47.66830N / 122.35385W	1976-2016
SnohoCty	SlvLk132	Silver Lk Water District	47.87685N / 122.20184W	1988-2016
ThurstonCty	59u	Bloody Run USGS	46.79028N / 122.73417W	2010-2015
ThurstonCty	27u	Boston Harbor	47.13611N / 122.90205W	2007-2016
ThurstonCty	60u	Bucoda USGS	46.77222N / 122.92306W	2010-2016
ThurstonCty	65u	Grand Mound	46.79429N / 123.02449W	2007-2016
ThurstonCty	33w	Griffin FS	47.08536N / 123.01648W	2009-2016
ThurstonCty	33x	Griffin FS 13-2	47.14990N / 122.94567W	2017-2017
ThurstonCty	32u	Kaiser Rd	47.07019N / 122.95583W	2004-2012
ThurstonCty	18u	Lacey Fire Dist 3FS	47.03678N / 122.81610W	2006-2016
ThurstonCty	45u	Littlerock	46.90223N / 123.02264W	2007-2016
ThurstonCty	13u	Lk Lawrence	46.85780N / 122.57851W	2007-2016
ThurstonCty	24u	McLane Black Lk FS 91	47.04601N / 122.97679W	2013-2016
ThurstonCty	10u	Meridian Rd	46.97402N / 122.73863W	2004-2016
ThurstonCty	23u	Percival Cr Bldg 4	47.02865N / 122.91413W	2002-2016
ThurstonCty	11w	Rainier TX FR Station	46.53559N / 122.41546W	2014-2016
ThurstonCty	45w	Rochester Drop Box	46.84762N / 123.04808W	2010-2016
ThurstonCty	20u	Southbay FS	47.08173N / 122.84514W	2007-2016
ThurstonCty	69u	Summit Lk	47.05085N / 123.13703W	2007-2016
ThurstonCty	55u	Tenino	46.86129N / 122.84066W	2007-2016
ThurstonCty	18w	WARCTC	47.06578N / 122.76009W	2003-2016
ThurstonCty	05u	Yelm WRF	46.95176N / 122.59726W	2009-2016